

F_N-Based Nodal Transport Method in X-Y Geometry

Ser Gi Hong and Nam Zin Cho
Korea Advanced Institute of Science and Technology
Department of Nuclear Engineering
373-1 Kusong-dong, Yusong-gu
Taejon, Korea 305-701

Abstract

A nodal transport method based on the F_N method is developed for the transport calculation in $x-y$ geometry and tested for benchmark problems. Using transverse integration, the two-dimensional transport equation is converted to one-dimensional equations for x, y -directions and the one-dimensional equations are integrated over azimuthal angle. With proper approximations for the transverse leakage, the one-dimensional equations are discretized by using the F_N method without truncation error. At present, isotropic approximation of the transverse with a quadratic or flat shape in spatial variable is tested.

I. Introduction

In the last few years, considerable progress has been made in the development of a certain class of nodal coarse-mesh methods in the transport theory. However, currently known nodal transport methods are not as accurate for transport problems as diffusion nodal methods are for diffusion problems. This is because the one-dimensional transverse integrated diffusion equations are solved analytically using an approximation only for the transverse leakage terms, whereas the one-dimensional transverse integrated transport equations are solved analytically using approximations for the transverse leakage and the scattering source term.

The F_N method was first developed by Siewert and Benoist^{1,2} and used to obtain concise and accurate results for the half space and the finite slab. The derivation of the F_N method starts with an equation that gives the analytic solution in terms of the infinite medium Green's function in infinite medium slab geometry and the infinite medium Green's function is represented by Case's bases³. The equation for the infinite medium is transformed to the equation for the finite slab by using Placzek lemma and projected onto Case's bases. The resulting equations are two singular integral equations in which the interface angular fluxes are unknowns. In the F_N method, the interface angular fluxes are expanded by polynomial basis. Therefore, the F_N method has no truncation error in spatial variable in slab geometry.

In this paper, an interface current nodal method is developed by using the well-known transverse integration procedure^{4,5} and by solving the one-dimensional equations with the F_N method, only approximating (in spatial variables) the transverse leakage; the scattering source terms in the one-dimensional equations are treated implicitly and exactly (in spatial variable). At present, isotropic approximation of the transverse with a quadratic shape in spatial variable is used. With those approximations of the transverse leakage, the polynomial expansion of the interface angular flux leads to a response matrix equation for one node. A one node block inversion method was used to solve the nodal equation. Numerical tests show that our method gives accurate solution in comparison to other methods.

II. Theory and Methodology

The starting point is the one-group transport equation with isotropic scattering and isotropic sources in $x-y$ geometry

$$\mu \frac{\partial \psi(x, y, \mathcal{D})}{\partial x} + \eta \frac{\partial \psi(x, y, \mathcal{D})}{\partial y} + \sigma \psi(x, y, \mathcal{D}) = \frac{\sigma_s}{4\pi} \int_{4\pi} d\Omega' \psi(x, y, \mathcal{D}') + S(x, y), \quad (1)$$

where S is the inhomogeneous source and σ is the total scattering cross section. Eq.(1) is transformed into two one-dimensional equations by the transverse integration procedure and the equations are integrated over azimuthal angle. The equation for x-direction is given by

$$\mu \frac{\partial \psi^x(x, \mu)}{\partial x} + \sigma \psi^x(x, \mu) - \frac{\sigma_s}{2} \int_{-1}^{+1} d\mu' \psi^x(x, \mu') = S^x + L_{ij}^x(x, \mu), \quad (2)$$

where the transverse leakage and the x-direction angular flux are given by

$$\begin{aligned} L_{ij}^x(x, \mu) &= \frac{1}{2\pi \Delta y_j} \int_0^{2\pi} d\varphi_x \eta [\psi(x, 0, \mu, \varphi_x) - \psi(x, \Delta y_j, \mu, \varphi_x)], \\ \psi^x(x, \mu) &= \frac{1}{2\pi \Delta y_j} \int_0^{\Delta y_j} dy \int_0^{2\pi} d\varphi_x \psi(x, y, \mu, \varphi_x). \end{aligned} \quad (3)$$

At present, the dependency of the transverse leakage on the azimuthal angle is ignored and the spatial distribution is assumed to be a quadratic shape

$$\begin{aligned} L_{ij}^x(x, \mu) &\cong \frac{1}{2} \int_{-1}^{+1} d\mu' L_{ij}^x(x, \mu') = L_{ij}^x(x) = \frac{F_{ij-1/2}^x(x) - F_{ij+1/2}^x(x)}{\Delta y_j}, \\ L_{ij}^x(x) &= \bar{L}_{ij}^x + (\bar{L}_{i-1j}^x - \bar{L}_{ij}^x) \rho_x^{i-1}(x) + (\bar{L}_{i+1j}^x - \bar{L}_{ij}^x) \rho_x^{i+1}(x), \end{aligned} \quad (4)$$

where the quadratic shape function $\rho(x)$ is the shape function in the analytic nodal method (ANM). For the nodal coupling equations, Eq.(2) and the counterpart for y-direction are discretized by the FN method :

$$\begin{aligned} &\int_0^1 \psi^x(x_{i-1/2}, -\mu) \mu \phi(\xi, \mu) d\mu + e^{-\sigma \Delta x_j / \xi} \int_0^1 d\mu \mu \psi^x(x_{i+1/2}, \mu) \phi(-\xi, \mu) \\ &= \int_0^1 \psi^x(x_{i-1/2}, \mu) \mu \phi(-\xi, \mu) d\mu + e^{-\sigma \Delta x_j / \xi} \int_0^1 d\mu \mu \psi^x(x_{i+1/2}, -\mu) \phi(\xi, \mu) \\ &+ \int_{-1}^{+1} d\mu \phi(-\xi, \mu) \int_0^{\Delta x_i} dx [S^x + L_{ij}^x] e^{-\sigma(x-x_{i-1/2})/\xi}, \end{aligned} \quad (5a)$$

$$\begin{aligned} &\int_0^1 \psi^x(x_{i+1/2}, \mu) \mu \phi(\xi, \mu) d\mu + e^{-\sigma \Delta x_j / \xi} \int_0^1 d\mu \mu \psi^x(x_{i-1/2}, -\mu) \phi(-\xi, \mu) \\ &= \int_0^1 \psi^x(x_{i+1/2}, -\mu) \mu \phi(-\xi, \mu) d\mu + e^{-\sigma \Delta x_j / \xi} \int_0^1 d\mu \mu \psi^x(x_{i-1/2}, \mu) \phi(\xi, \mu) \\ &+ \int_{-1}^{+1} d\mu \phi(\xi, \mu) \int_0^{\Delta x_i} dx [S^x + L_{ij}^x] e^{-\sigma(x_{i+1/2}-x)/\xi}, \end{aligned} \quad (5b)$$

where the Case's eigenfunction of the transport equation is given by

$$\begin{aligned} \phi(\nu_0, \mu) &= \frac{c\nu_0}{2} \frac{1}{\nu_0 - \mu}, \quad 1 - \frac{c\nu_0}{2} \log \frac{\nu_0 + 1}{\nu_0 - 1} = 0, \\ \phi(\nu, \mu) &= \frac{c\nu}{2} P\nu \left(\frac{1}{\nu - \mu} \right) + \lambda(\nu) \delta(\nu - \mu), \quad \nu \in (-1, 1). \end{aligned} \quad (6)$$

and in Eq.(6), Pv represents the Cauchy principal value. Then, the interface angular fluxes in Eq.(5) are expanded by a polynomial. For example, incoming flux in left side is expanded as follows :

$$\psi^x(x_{i-1/2}, \mu) = \sum_{\alpha=0}^N \phi_{i-1/2}^{x,+} \mu^\alpha. \quad (7)$$

By substituting the above expanded interface angular fluxes into Eq.(5), the following nodal coupling equations are obtained :

$$\begin{aligned} & \sum_{\alpha=0}^N B_{\alpha, ij}(\xi_\beta) \phi_{i-1/2, \alpha}^{x,-} + e^{-\sigma \Delta x_i / \xi_\beta} \sum_{\alpha=0}^N A_{\alpha, ij}(\xi_\beta) \phi_{i+1/2, \alpha}^{x,+} \\ &= \sum_{\alpha=0}^N A_{0, ij}(\xi_\beta) \phi_{i-1/2, \alpha}^{x,+} + e^{-\sigma \Delta x_i / \xi_\beta} \sum_{\alpha=0}^N B_{\alpha, ij}(\xi_\beta) \phi_{i+1/2, \alpha}^{x,-} \\ &+ \frac{2}{c \xi_\beta} \int_{x_{i-1/2}}^{x_{i+1/2}} dx \{ S^x + A_{ij}^x + B_{ij}^x \left(\frac{x - x_{i-1/2}}{\Delta x_i} \right) + C_{ij}^x \left(\frac{x - x_{i-1/2}}{\Delta x_i} \right)^2 \} e^{-\sigma(x - x_{i-1/2}) / \xi_\beta}, \end{aligned} \quad (8a)$$

$$\begin{aligned} & \sum_{\alpha=0}^N B_{\alpha, ij}(\xi_\beta) \phi_{i+1/2, \alpha}^{x,+} + e^{-\sigma \Delta x_i / \xi_\beta} \sum_{\alpha=0}^N A_{\alpha, ij}(\xi_\beta) \phi_{i-1/2, \alpha}^{x,-} \\ &= \sum_{\alpha=0}^N A_{0, ij}(\xi_\beta) \phi_{i+1/2, \alpha}^{x,-} + e^{-\sigma \Delta x_i / \xi_\beta} \sum_{\alpha=0}^N B_{\alpha, ij}(\xi_\beta) \phi_{i-1/2, \alpha}^{x,+} \\ &+ \frac{2}{c \xi_\beta} \int_{x_{i-1/2}}^{x_{i+1/2}} dx \{ S^x + A_{ij}^x + B_{ij}^x \left(\frac{x - x_{i-1/2}}{\Delta x_i} \right) + C_{ij}^x \left(\frac{x - x_{i-1/2}}{\Delta x_i} \right)^2 \} e^{-\sigma(x_{i+1/2} - x) / \xi_\beta}, \end{aligned} \quad (8b)$$

where the coefficients A_α, B_α are given as follows :

$$\begin{aligned} A_\alpha(\xi) &= \frac{2}{c \xi} \int_0^1 \mu^{\alpha+1} \phi(-\xi, \mu) d\mu, \\ B_\alpha(\xi) &= \frac{2}{c \xi} \int_0^1 \mu^{\alpha+1} \phi(\xi, \mu) d\mu, \end{aligned} \quad (9)$$

and $A_{ij}^x, B_{ij}^x, C_{ij}^x$ are functions of (ij)'th node average transverse leakage, (i-1j)'th node average transverse leakage, and (i+1j)'th node average transverse leakage. Since the transverse leakages are related with the interface currents, the equation of relating the interface currents with the nodal unknowns is required. The equation is obtained with the definition of the interface current :

$$\begin{aligned} J_{i+1/2}^x &= \frac{1}{2} \int_{-1}^{+1} d\mu \mu \psi^x(x_{i+1/2}, \mu) \\ &= \frac{1}{2} \int_0^1 d\mu \mu \psi^x(x_{i+1/2}, \mu) - \frac{1}{2} \int_0^1 d\mu \mu \psi^x(x_{i+1/2}, -\mu) \\ &= \frac{1}{2} \sum_{\alpha=0}^N \frac{\phi_{i+1/2, \alpha}^{x,+}}{\alpha+2} - \frac{1}{2} \sum_{\alpha=0}^N \frac{\phi_{i+1/2, \alpha}^{x,-}}{\alpha+2}. \end{aligned} \quad (10)$$

Substituting Eq.(10) into Eq.(8), the derivation of the nodal coupling equations is completed and the equation can be written in the following vector form for one node :

$$\mathbf{A}^- \vec{\Psi}^{out} = \mathbf{B}^- \vec{\Psi}^{in} + \vec{R}, \quad (11)$$

where \vec{R} includes the inhomogeneous sources and the interface nodal unknowns of adjacent nodes, and the matrices \mathbf{A}, \mathbf{B} are given as follows :

$$\mathbf{A} = \begin{bmatrix} \mathbf{A}^x & \mathbf{A}^y \\ \mathbf{A}^y & \mathbf{A}^x \end{bmatrix}, \quad \mathbf{B} = \begin{bmatrix} \mathbf{B}^x & \mathbf{B}^y \\ \mathbf{B}^y & \mathbf{B}^x \end{bmatrix}. \quad (12)$$

The above nodal coupling equation is solved by a one node block inversion method. In the one node block inversion method, first, all incoming fluxes for each node are assumed to be known and then Eq.(11) for each node are directly inverted by Gaussian elimination. Our experience indicates that the spectral radius of this iteration method is smaller than that of the scattering source iteration method.

III. Applications and Numerical Results

For verification of the F_N nodal method, two benchmark problems are chosen. The first benchmark problem is shown in Fig. 1. This problem is selected from Ref. 6 and solved with three types of mesh divisions (4x4, 10x10, 20x20). The converged solution with a pointwise relative convergence criterion of $10E-4$ is used to calculate the quadrant-averaged scalar fluxes and the average scalar flux for the detector region. To compare our results, the results from Ref. 6 are used. In Ref. 6, the linear nodal (LN) method, the linear-linear (LL) nodal method, and the bilinear (BL) method are tested with S_4 angular quadrature set and with the same convergence criterion as ours. F_1 is used in this problem. The results of the TWODANT code⁷ with a fine mesh division (100x100) are also compared. The results are summarized in Table I. In comparison with the results of the TWODANT code, the results show that our method gives more accurate solutions than the three nodal methods in Ref. 6 for the region I, II and the detector region, but the solutions of the three nodal methods are more accurate than that of our method for the region IV. It is also noted that the results with flat shape of the transverse leakage are comparable to those with quadratic shape of the transverse leakage and that the number of calculated negative fluxes for our method is fewer than those for the three nodal methods in Ref. 6.

Table I Comparison of the numerical solutions for benchmark problem I

Mesh	Method	I	II	IV	Detector	Number of negative fluxes
4x4	F_1 (flat)	1.6879E+00	0.4013E-01	0.1062E-02		0
	F_1 (quadratic)	1.6840E+00	0.4104E-01	0.1871E-02		3
10x10	F_1 (flat)	1.6861E+00	0.4051E-01	0.1580E-02	0.2024E+00	0
	F_1 (quadratic)	1.6847E+00	0.4090E-01	0.1171E-02	0.2025E+00	1
	LN	1.676E+00	0.4170E-01	0.1986E-02	0.2151E+00	8
	LL	1.676E+00	0.4170E-01	0.1989E-02	0.2151E+00	6
	BL	1.676E+00	0.4170E-01	0.1996E-02	0.2151E+00	6
20x20	F_1 (flat)	1.6854E+00	0.4071E-01	0.1389E-02	0.2024E+00	0
	F_1 (quadratic)	1.6848E+00	0.4087E-01	0.1199E-02	0.2025E+00	0
	LN	1.676E+00	0.4161E-01	0.1990E-02	0.2145E+00	16
	LL	1.676E+00	0.4161E-01	0.1991E-02	0.2145E+00	18
	BL	1.676E+00	0.4160E-01	0.1992E-02	0.2145E+00	18
TWODANT (100x100, S_4)		1.6852E+00	0.4056E-01	0.1739E-02	0.2054E+00	

Benchmark problem II is devised to numerically analyze the effects of the shapes of the transverse leakage. Since all the boundary conditions are vacuum, the leakages through the external boundaries are very important. The definition of the benchmark problem is described in Fig. 2. The results are given in Table II. In this calculation, the result of the TWODANT code with fine mesh division (100x100) is used as reference solution and F_3 is used in our method. Our results for flat and quadratic shape of the transverse leakage are very accurate except in the two nodes that are located in top corners. It is also noted that the errors in source regions are nearly equal to zero.

Table II Absolute relative errors(%) for benchmark problem II

1.5054(a)	2.6886	2.4269	1.2727	0.3186
5.626(b)	1.190	1.989	0.887	6.001
2.152(c)	0.402	0.688	0.369	2.096
2.809(d)	0.866	0.614	1.257	2.325
1.302(e)	0.412	0.486	0.345	1.262
14.306	19.282	17.809	7.3608	
1.418	0.108	0.819	0.384	
0.768	0.021	0.348	0.059	
1.712	0.176	0.348	1.643	
0.803	0.041	0.269	0.516	
46.869	49.381	48.661		
0.064	0.002	0.022		
0.029	0.002	0.008		
0.015	0.002	0.002		
0.015	0.000	0.006		
47.608	50.000			
0.002	0.000			
0.002	0.000			
0.004	0.000			
0.002	0.000			
45.397				
0.057				
0.039				
0.024				
0.019				

- (a) reference flux : TWODANT (S_{16}), 100x100 mesh division
 (b) with flat transverse shape and 10x10 mesh division
 (c) with flat transverse shape and 15x15 mesh division
 (d) with quadratic transverse shape and 10x10 mesh division
 (e) with quadratic transverse shape and 15x15 mesh division

IV. Conclusions and Discussion

In this paper, a nodal transport method based on the F_N method is developed for the transport calculation in $x-y$ geometry and tested for benchmark problems. For verification of our method, the results are compared with other methods. The transverse integration procedure is used to derive the one-dimensional equations and the equations are integrated over the azimuthal angle. The nodal coupling equations are derived by solving the one-dimensional equations with the F_N method that has no truncation error for spatial variable in slab geometry. The numerical results show that our method gives accurate solutions except in the external regions. It is considered that the larger error in the outside regions is due to the assumption of the isotropic transverse leakage. The extension to the three-dimensional geometry is straightforward. We plan to study the extensions of the F_N nodal method to the multigroup, eigenvalue problem and anisotropy of the transverse leakage in the future.

References

1. C. E. Siewert and P. Benoist, "The F_N Method in Neutron Transport Theory. Part I: Theory and Applications," Nucl. Sci. Eng., **69**, 156-160 (1979).
2. C. E. Siewert and P. Benoist, "The F_N Method in Neutron Transport Theory. Part II: Applications and Numerical Results," Nucl. Sci. Eng., **69**, 161-168 (1979).
3. K. M. Case and P. F. Zweifel, *Linear Transport Theory*, Addison-wesley Publishing Co., Inc., Reading, Massachusetts (1967).
4. M. R. Wagner, "A Nodal Discrete-Ordinates Method for the Numerical Solution of the Multi-Dimensional Transport Equation," *Proceedings of the Topical Meeting on Computational Methods in Nuclear Engineering, Williamsburg, VA*, Vol. 2, p. 4.117,

American Nuclear Society (1979).

5. R. D. Lawrence, "Three-Dimensional Nodal Diffusion and Transport Methods for The Analysis of Fast-Reactor Critical Experiments," Progress in Nuclear Energy, Vol. 18, No. 1/2, pp. 101-111, 1986
6. Y. Y. Azmy, "Comparison of Three Approximations to the Linear-Linear Nodal Transport Method in Weighted Diamond-Difference Form," Nucl. Sci. Eng., 100, 190-200 (1988).
7. R. E. Alcouffe et al., "User's Guide for TWODANT: A Code Package for Two-Dimensional, Diffusion-Accelerated, Neutral-Particle Transport," LA-10049-M, Los Alamos National Laboratory(1990).

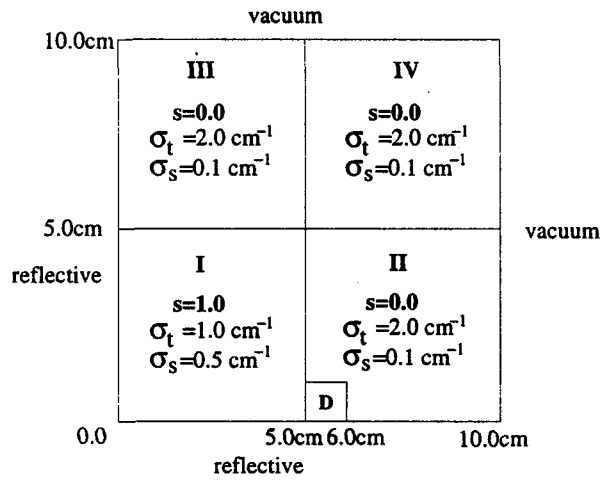


Fig. 1. Geometry and cross sections for the benchmark problem I

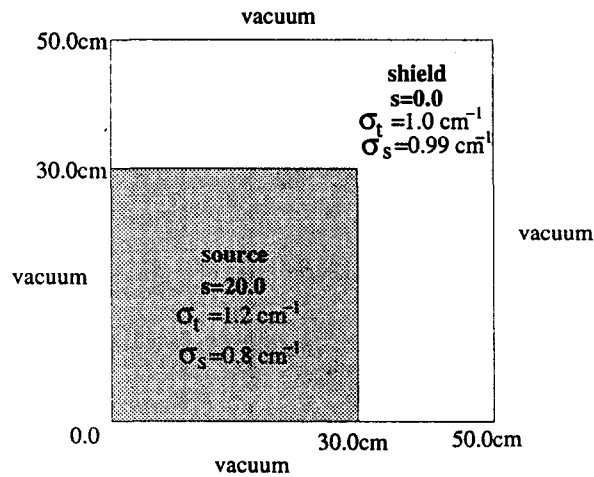


Fig. 2. Geometry and cross sections for the benchmark problem II